Accepted Manuscript

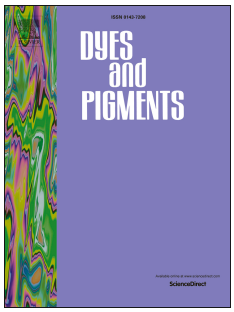

Near-Infrared Absorbing Dyes at 1064nm: Soluble Dithiolene Nickel Complexes with Alkylated Electron-Donating Groups as Peripheral Substituents

Dr. Yingliang Liu, Zhenru Zhang, Xuemei Chen, Shengang Xu, Prof. Shaokui Cao

PII: S0143-7208(16)00038-3

DOI: 10.1016/j.dyepig.2016.01.026

Reference: DYPI 5080

To appear in: *Dyes and Pigments*

Received Date: 4 August 2015

Revised Date: 1 January 2016

Accepted Date: 5 January 2016

Please cite this article as: Yingliang Liu Zhang Z, Chen X, Xu S, Shaokui Cao Near-Infrared Absorbing Dyes at 1064nm: Soluble Dithiolene Nickel Complexes with Alkylated Electron-Donating Groups as Peripheral Substituents, *Dyes and Pigments* (2016), doi: 10.1016/j.dyepig.2016.01.026.

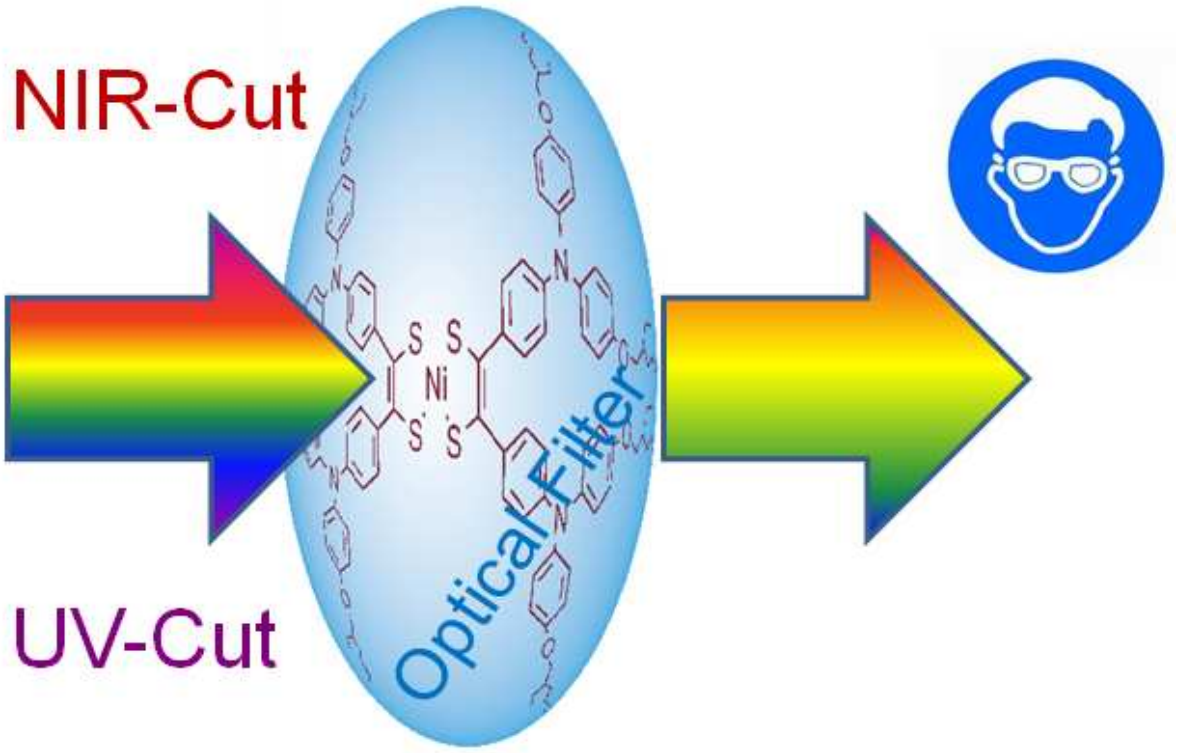

Near-Infrared Absorbing Dyes at 1064nm: Soluble Dithiolene Nickel Complexes with Alkylated Electron-Donating Groups as Peripheral Substituents

Yingliang Liu,* Zhenru Zhang, Xuemei Chen, Shengang Xu, Shaokui Cao*

School of Materials Science and Engineering, Zhengzhou University, Zhengzhou 450052, P. R. China

ABSTRACT

Soluble dithiolene nickel complexes are designed and synthesized as near-infrared (NIR) absorbing dyes through the introduction of strong electron-donating groups at the molecular periphery. The resulting complexes are characterized by $^{1}H/^{13}C$-NMR, IR, ESI-MS, UV-vis-NIR, TG, DSC, XPS and elemental analysis. The identification results are in accord with the chemical structure of designed dithiolene nickel complexes. The XPS results suggested that the dithiolene ligands in carbazole-containing nickel complex take a radical monoanion, which depends on the substituent electron-donating ability to a large extent. The TG and DSC measurements indicated that the resulting complexes have an excellent thermal stability and take on a glassy state at low temperature. The laser transmittance measurement suggested that the optical filters fabricated through static solution-casting approach with dithiolene nickel complexes as NIR absorbing dyes could be well applied to the NIR laser protection at 1064 nm.

Keyword: near-infrared; absorbing dye; dithiolene nickel complex; laser protection

1. INTRODUCTION

* Correspondence to: Dr. Yingliang Liu, liuylxn@sohu.com; Prof. Shaokui Cao, caoshaokui@zzu.edu.cn. Tel.&Fax: +86-371-6776-3523.

The near-infrared (NIR) optical filtering will be paid much more attention with the rapid development of laser applications in biological medicine[1, 2], free-space optical telecommunication[3], satellite remote sensing[4, 5], night view imaging[6] and other military fields[7]. Especially, the NIR optical filtering in relation with optical attenuation and laser protection within biological optical window of 800~1300nm, which is derived from the total transmittance of blood and water[8], becomes an important issue[9] in the process of medical imaging[10], NIR medical therapeutics[11] and NIR-controlled drug release[12-16]. Additionally, the NIR optical filtering is also specially emphasized in all kinds of military activities because many military lasers work within the NIR wavelength range, such as the laser at 1064nm[17-20].

The optical filtering, which are often applied in laser protections, photographs, precision instruments, eye-protecting glasses, etc., are usually achieved from absorbing dyes[19], nonlinear refringence/scattering materials[21], photonic crystals[22, 23], interference/diffraction gratings[24], dichroic/dielectric reflections[25, 26], phase changes, and so on. One of them, the absorbing dyes are one of the most promising optical filtering materials suitable for the convenient processing approach, for example, static casting or injection molding, which will avoid the complicated fabrication processes of high precision patterns, such as gratings, photonic crystals, etc. Currently, the well-known dye categories include metal complexes, cyanines, porphyrins, phthalocyanines, quinoids, azo compounds, etc[17]. Thereamong, dithiolene metal complexes have been applied to NIR photodetector, dye sensitized solar cells, field effect transistor, second/third-order optical nonlinearity, Q-switch dye lasers, antioxidants for polymers and light stabilizers on account of high electron mobility, superior photostability, air-stability and thermal stability[27, 28]. Due to their tense and broad absorption in the near-infrared region, dithiolene metal complexes are also a kind of quite outstanding NIR optical filtering materials. Interestingly, a certain transmittance in visible light region of dithiolene metal complexes affords the potential combination of NIR laser protection and visibility in the visible region. More interestingly, the transparent region of dithiolene metal complexes has the potential to be red-shifted to the working wavelength of low-light night view devices.

For example, the NVIS-compatible optical filter in the NIR range of 700-1000nm has been reported with an aim to filtrate the interferential light of light-emitting device in martial applications[18]. However, its NIR optical filtering range is not yet in accord with biological optical window of 800-1300nm, eliminating the disturbance of heterochromatic light or being used for the laser protection within biological optical window.

Soluble dithiolene nickel complexes are designed and synthesized in this work as NIR absorbing dyes through the introduction of strong electron-donating groups at the molecular periphery, such as *N*-(2-ethylhexanyl)carbazol-3-yl, *N*-(2-ethylhexanyl)phenothiazin-3-yl and *N*, *N*-bis[(4-(2-ethylhexyloxy)phenyl]-anilin-4-yl groups, to red-shift the NIR optical filtering range of dithiolene nickel complexes to biological optical window. The introduction of *N*-(2-ethylhexanyl) group is to increase the dye solubility. The resulting complexes are characterized by $^{1}H/^{13}C$-NMR, IR, ESI-MS, UV-vis-NIR and XPS spectra, together with TG, DSC and CV. The NIR absorbing filters are fabricated through static solution-casting approach with polystyrene as transparent polymeric matrix and with dithiolene nickel complexes as NIR absorbing dyes. Their laser transmittance measurement suggested that the fabricated NIR absorbing filters could be applied to the NIR optical filtering in biological optical window, especially the NIR laser protection at 1064nm.

2. Experimental Section

2.1. Reagents: Nickel chloride hexahydrate ($NiCl_2 \cdot 6H_2O$) is bought from AlfaAesar Chemical Co. Ltd. 1-Bromo-2-ethylhexane, ethanedioyl chloride and phosphorus pentasulfide are purchased from Aladdin Chemical Co. Ltd. Carbazole, phenothiazine and *N*-bromosuccinimide are bought from Zhengzhou alpha chemical Co. Ltd. 4-Iodophenol is from J&K Scientific Ltd. 4-Bromoanilines is from AlfaAesar. Other reagents and solvents are from Chinese chemical companies. All the reagents are directly used without further purification. *N*, *N*-Dimethyl formamide (DMF) is dried overnight with anhydrous magnesium sulfate and then refluxed over calcium hydride

for 12 hours. Toluene and dioxane are dried overnight with anhydrous magnesium sulfate and then refluxed over sodium for 4 hours with benzophenone as an indicator. Dichloromethane is dried by refluxing over phosphorous pentoxide for 4 hours.

2.2. Instruments and Characterization: ^{1}H-/^{13}C-NMR spectra are recorded on Bruker DPX-400 nuclear magnetic resonance spectrometer using *d*-chloroform or *d*-dimethylsulphoxide solution at room temperature. Infrared (IR) spectra are measured using Nicolet Protégé 460 Infrared Spectrometer. ESI-MS is performed on APEX IV fourier transform ion cyclotron resonance mass spectrameter. Thermogravimetry (TG) is investigated on NETZSCH TG-209 Thermogravimetric Analyzer at heating and cooling rates of 10^{o}C/min under N_2 atmosphere. Differentionial scanning calorimetry (DSC) is carried out with NETZSCH-DSC-204 Differential Scanning Calorimeter at heating and cooling rates of 10^{o}C/min under N_2 atmosphere. Ultraviolet-visible-NIR (UV-vis-NIR) spectra are recorded using the quartz cuvette with a thickness of 1cm on Agilent Cary5000 Spectrophotometer. Cyclic voltammetry is carried out on CHI600E electrochemical working station at a scanning rate of 100mv/s. The transmitted laser power of fabricated optical filters is measured by an optical powermeter with the NIR lasers (780, 1064 and 1550 nm) as an incidence light source.

2.3. Synthesis: All the intermediates and dithiolene nickel complexes are synthesized according to the synthetic route in **Scheme 1**.

***N*-(2-Ethylhexyl)-carbazole (1)**: A 250mL round-bottomed flask is charged with carbazole (15.1g, 90mmol) and DMF (130mL). NaH (2.59g, 108mmol) is slowly added when carbazole is completely dissolved. The resulting mixture is stirred for 30 minutes. Then, 2-ethylhexylbromide（20.86g，108mmol）is added under argon and stirred overnight at room temperature. The reaction is quenched with 300 mL of distilled water and extracted three times with *n*-hexane (80mL each). Organic combined fraction is washed with brine and dried over anhydrous $MgSO_4$. The solvent is removed under reduced pressure and the residue is purified by silica column chromatography using *n*-hexane as eluent. *N*-(2-Ethylhexyl)-carbazole is obtained as a

colorless viscous liquid in the yield of 90.2%. ^{1}H-NMR (400MHz, $CDCl_3$, δ): 8.12 (d, *J*=7.76Hz, 2H), 7.47 (t, *J*=7.32Hz, 2H), 7.42 (d, *J*=8.16Hz, 2H), 7.24 (t, *J*=7.08Hz, 2H), 4.17 (d, *J*=4.32Hz, 2H), 2.09 (m, 1H), 1.23-1.48 (m, 8H), 0.90 (dt, *J*=7.40, 7.08Hz, 6H). IR, υ_{max} (KBr, cm^{-1}): 3054 (ArH), 2958 (CH_3, υ_{as}), 2927 (CH_2, υ_{as}), 2857 (CH_2, υ_s), 1598, 1571, 1484, 1463 (benzene ring), 1452 (CH_3, υ_{as}), 1152 (C-N), 748 (*o*-substitution).

1,2-Bis[*N*-(2-ethylhexyl)-carbazol-3-yl]ethane-1,2-dione (2): Compound 1 (5.03g, 18mmol) and oxalyl chloride (0.73mL, 7.5mmol) are added in turn into a 100mL three-necked round-bottomed flask charged with anhydrous CH_2Cl_2 (20mL). $AlCl_3$ (2.8g, 21mmol) is added slowly to the mixture at 0^{o}C. The reaction mixture is stirred for 8 hours at ambient temperature and then quenched with ice and concentrated HCl. After stirring for another one hour, organic layer is separated and aqueous layer is extracted with dichloromethane. The combined organic layer is washed with distilled water and dried over anhydrous $MgSO_4$. After evaporating the solvent, the resulting residue is purified using column chromatography (silica gel, chloroform) to provide a yellow solid in the yield of 43.1%. ^{1}H-NMR (400 MHz, $CDCl_3$, δ): 8.80 (s, 2H), 8.21 (d, *J*=7.96Hz, 2H), 8.05 (d, *J*=7.76Hz, 2H), 7.46 (t, *J*=7.46Hz, 2H), 7.38 (t, *J*=8.92Hz, 4H), 7.24 (d, *J*=7.52Hz, 2H), 4.10 (d, *J*=7.16Hz, 4H), 2.01 (t, *J*=5.96Hz, 2H), 1.20-1.38 (m, 16H), 0.87 (t, *J*=7.32Hz, 6H), 0.83 (t, *J*=7.00Hz, 6H). ^{13}C-NMR (101MHz, $CDCl_3$, δ): 195.08 (s) (carbonyl groups), 144.48 (s), 141.54 (s), 127.66 (s), 126.63 (s), 124.79 (s), 123.90 (s), 122.94 (s), 120.73 (s), 120.28 (s), 109.64 (s), 109.15 (s) (carbazole), 47.53 (s), 39.29 (s), 30.88(s), 28.69(s), 24.29(s), 22.93(s), 13.96(s), 10.81(s) (2-ethylhexanyl groups). IR, υ_{max} (KBr, cm^{-1}): 3053 (ArH), 2957 (CH_3, υ_{as}), 2922 (CH_2, υ_{as}), 2863 (CH_2, υ_s), 1669 (C=O), 1592, 1507, 1464 (benzene ring), 1336 (CH_2, υ_s), 1157 (C-N), 833 (*m*-substitution). ESI-MS (m/z): [M+1]=613.4.

Bis{1,2-bis[*N*-(2-ethylhexyl)-carbazol-3-yl]ethylene-1,2-ditholate} nickel complex (3): Compound 2 (1. 19g，5mmol) is refluxed at 95^{o}C with P_2S_5 (3.33g, 15mmol) in 20ml of dioxane for 10 hours. The reaction mixture is filtered to remove the excess P_2S_5. A solution of $NiCl_2 \cdot 6H_2O$ (0.58g, 2.5mmol) in distilled water (3ml) is added to

the filtrate. The mixture is refluxed at 85°C for 4 hours. After cooling, the reactant is poured into distilled water (20mL) and extracted for three times with dichloromethane. The combined organic fraction is washed with brine and dried over anhydrous $MgSO_4$. The solvent is removed under reduced pressure and the residue is purified by column chromatography using silica gel and dichloromethane as eluent to give a blackish green solid in the yield of 40.2%. ^{1}H-NMR (400MHz, $CDCl_3$, δ): 8.48 (s, 4H), 8.02 (d, *J*=7.68Hz, 4H), 7.47 (t, *J*=7.64Hz, 4H), 7.39 (t, *J*=7.88Hz, 8H), 7.23 (t, *J*=7.36Hz, 4H), 7.17 (d, *J*=8.64Hz, 4H), 4.13 (d, *J*=6.92Hz, 8H), 2.05 (m, 4H), 1.21-1.36 (m, 32H), 0.88 (dt, *J*=7.28, 7.12Hz, 24H). ^{13}C-NMR (101MHz, $CDCl_3$, δ): 181.80 (s) (C=C), 141.76 (s), 14161 (s), 133.77 (s), 127.42 (s), 126.32 (s), 123.47 (s), 123.42 (s), 122.01 (s), 121.06 (s), 119.73 (s), 109.60 (s), 108.93 (s) (carbazole), 47.97 (s), 39.74 (s), 31.37 (s), 29.14 (s), 24.76 (s), 23.41 (s), 14.41 (s), 11.25 (s) (2-ethylhexanyl groups). IR, υ_{max} (KBr, cm^{-1}): 3050 (ArH), 2957 (CH_3, υ_{as}), 2922 (CH_2, υ_{as}), 2855 (CH_2, υ_s), 1617, 1591, 1473 (benzene ring), 1336 (CH_2, υ_s), 1268, 1217 (C=C), 1123 (C-N), 902 (*m*-substitution), 749 (*o*-substitution). ESI-MS (m/z): [M+1]=1347.6. Element. Anal. Calcd for $C_{84}N_4S_4H_{96}Ni$: C, 74.83; N, 4.16; H, 7.13. Found: C, 74.40; N, 3.84; H, 7.23.

***N*-(2-Ethylhexyl)-phenothiazine (4):** A 250 mL Schlenk flask is charged with phenothiazine (18.0g, 90mmol), NaH (2.81g, 117mmol) and 100mL of DMF. The resulting mixture is stirred for 30 minutes. 2-Ethylhexylbromide (22.7g, 117mmol) is then added. The mixture is stirred overnight at room temperature. The reaction is quenched with distilled water and extracted for three times with *n*-hexane. The combined organic fraction is washed with brine and dried over anhydrous $MgSO_4$. The solvent is removed under reduced pressure and the residue is purified by column chromatography using silica gel and *n*-hexane as eluent to give *N*-(2-ethylhexyl)-phenothiazine as a yellow viscous liquid in the yield of 86.8%. ^{1}H-NMR (400MHz, $CDCl_3$, δ): 7.15 (t, *J*=7.44Hz, 4H), 6.90 (p, *J*=7.44Hz, 4H), 3.73 (d, *J*=6.72Hz, 2H), 1.95 (m, 1H), 1.27–1.47 (m, 8H), 0.88 (m, 6H). IR, υ_{max} (KBr, cm^{-1}): 3065 (ArH), 2958 (CH_3, υ_{as}), 2927 (CH_2, υ_{as}), 2857 (CH_2, υ_s), 1593, 1485, 1458 (benzene ring), 1222 (C-N), 749 (*o*-substitution).

1,2-Bis[*N*-(2-ethylhexyl)-phenothiazin-3-yl]ethane-1,2-dione (5): Aromatic 1,2-diketone derived from *N*-(2-ethylhexyl)-phenothiazine, Compound 5, is synthesized according to the same procedure as Compound 2. The product is separated by column chromatography and chloroform as eluent to obtain a blackish green solid in the yield of 32.3%. ^{1}H-NMR (400MHz, $CDCl_3$, δ): 7.72 (d, *J*=8.52Hz, 2H), 7.71 (s, 2H), 7.16 (t, *J*=8.24Hz, 2H), 7.00 (d, *J*=7.60Hz, 2H), 6.97 (t, *J*=7.52Hz, 2H), 6.88 (d, *J*=7.92Hz, 4H), 3.77 (d, *J*=7.04Hz, 4H), 1.91 (m, 2H), 1.36-1.44 (m, 8H), 1.25 (m, 8H), 0.86 (m, 12H). ^{13}C-NMR (101MHz, $CDCl_3$, δ): 192.50 (s) (carbonyl groups), 151.83 (s), 143.86 (s), 130.24 (s), 129.07 (s), 127.81 (s), 127.51 (s), 1.27.42 (2), 126.03 (s), 124.87 (s), 123.76 (s), 116.64 (s), 115.36 (s) (phonothiazine), 51.46 (s), 36.04 (s), 30.61 (s), 28.52 (s), 23.92 (s), 23.04 (s), 14.01 (s), 10.45 (s) (2-ethylhexanyl groups). IR, υ_{max} (KBr, cm^{-1}): 3056 (ArH), 2966 (CH_3, υ_{as}), 2922 (CH_2, υ_{as}), 2856 (CH_2, υ_s), 1659 (C=O), 1592, 1570, 1547, 1459 (benzene ring), 1192 (C-N), 747 (*o*-substitution). ESI-MS (m/z): [M+1]=677.3.

Bis{1,2-bis[*N*-(2-ethylhexyl)-phenothiazin-3-yl]ethylene-1,2-ditholate} nickel complex (6): Dithiolene nickel complex derived from phonothiazine, Compound 6, is synthesized according to the same procedure as Compound 3. The product is purified by column chromatography using silica gel and dichloromethane as the eluent to give a blackish green solid in the yield of 17.6%. ^{1}H-NMR (400MHz, $CDCl_3$, δ): 7.40 (s, 4H), 7.16 (t, *J*=7.08Hz, 4H), 7.12 (d, *J*=7.64Hz, 4H), 7.01 (d, *J*=8.44Hz, 4H), 6.96 (t, *J*=7.4 Hz, 4H), 6.89 (d, *J*=8.08Hz, 4H), 6.69 (d, *J*=8.60Hz, 4H), 3.71 (d, *J*=6.88Hz, 8H), 1.93 (m, 4H), 1.37-1.46 (m, 32H), 1.27 (m, 24H). ^{13}C-NMR (101MHz, $CDCl_3$, δ): 179.32 (s) (carbonyl groups), 146.52 (s), 144.90 (s), 135.70 (s), 128.00 (s), 127. 86 (s), 127.67 (s), 127.20 (s), 125.88 (s), 125.22 (s), 122.80 (s), 116.02 (s), 115.32 (s) (phonothiazine), 51.20 (s), 35.84(s), 30.66 (s), 28.53 (s), 23.98 (s), 23.05 (s), 14.04 (s), 10.53 (s) (2-ethylhexanyl groups). IR, υ_{max} (KBr, cm^{-1}): 3068 (ArH), 2957 (CH_3, υ_{as}), 2915 (CH_2, υ_{as}), 2854 (CH_2, υ_s), 1591, 1566, 1559, 1456 (benzene ring), 1336 (CH_2, υ_s), 1268, 1242 (C=C), 1131 (C-N), 740 (*o*-substitution). ESI-MS (m/z): [M+2]=1476.5. Element. Anal. Calcd for $C_{84}N_4S_8H_{96}Ni$: C, 68.34; N, 3.80; H, 6.51. Found: C, 67.82; N, 3.35; H, 6.83.

1-(2-Ethylhexyloxy)-4-iodobenzene (7): K_2CO_3 (26.3g, 190mmol) is suspended in DMF (100mL), followed by the addition of 4-iodophenol (28.0g, 127mmol) and 2-ethylhexylbromide (26.6g, 135mmol). The mixture is refluxed for 51 hours under the protection of argon. The reaction is quenched with distilled water and extracted for three times with *n*-hexane. The combined organic fraction is washed with brine and dried over anhydrous $MgSO_4$. The solvent is removed under reduced pressure and the residue is purified by column chromatography using silica gel and *n*-hexane as eluent to give a colorless liquid in the yield of 76.7%. ^{1}H-NMR (400MHz, $CDCl_3$, δ): 7.51 (d, *J*=8.96Hz, 2H), 6.67 (d, *J*=8.96Hz, 2H), 3.78 (d, *J*=5.84Hz, 2H), 1.69 (m, 1H), 1.23-1.52 (m, 8H), 0.90 (m, 6H). IR, υ_{max} (KBr, cm^{-1}): 2958 (CH_3, υ_{as}), 2927 (CH_2, υ_{as}), 2872 (CH_2, υ_s), 1586, 1487, 1467 (benzene ring), 1283, 1244 (C-O-C), 1032 (C-O), 819 (*p*-substitution).

***N*-Bis[4-(2-ethylhexyloxy)phenyl] phenylaniline (8):** The reaction is carried out in a 250mL three-neck round-bottomed flask. Toluene (150mL) is charged to the round-bottom flask, followed by the addition of Compound 7 (35.6g, 107mmol), CuI (0.35g, 1.82mmol), 1,10-phenanthroline monohydrate (0.36g, 1.82mmol), aniline (4.75g, 51mmol), and KOt-Bu (17.1g, 153mmol). The round-bottom flask is flushed with argon for three times to ensure the removal of air. Then, an argon balloon is attached to the condenser to maintain the argon atmosphere during the reaction. The mixture is stirred at 115°C for 4 hours. After cooling to room temperature, the reaction mixture is quenched with distilled water (150mL) and extracted with toluene for three times. The combined organic fraction is washed with brine and dried over anhydrous $MgSO_4$. The solvent is removed under reduced pressure and the residue is separated by column chromatography and cyclohexane as eluent to obtain the product as a light yellow solid in the yield of 73.6%. ^{1}H-NMR (400MHz, $CDCl_3$, δ): 7.25 (d, *J*=7.48Hz, 2H), 7.13 (d, *J*=7.24Hz, 4H), 7.06 (d, *J*=7.64Hz, 2H), 6.93 (d, *J*=8.80Hz, 5H), 3.93 (d, *J*=5.12Hz, 4H), 1.84 (m, 2H), 1.39-1.69 (m, 16H), 1.06 (m, 12H). ^{13}C-NMR (101MHz, $CDCl_3$, δ): 155.68 (s), 149.01 (s), 141.07 (s), 128.99 (s), 126.52 (s), 120.93 (s), 120.50 (s), 115.35 (s) (benzene), 70.79 (s), 39.64 (s), 30.73 (s), 29.28 (s), 24.06 (s), 23.22 (s), 14.25 (s), 11.31 (s) (2-ethylhexanyl groups). IR, υ_{max} (KBr,

cm^{-1}): 3038 (ArH), 2957 (CH_3, υ_{as}), 2924 (CH_2, υ_{as}), 2871, 2858 (CH_2, υ_s), 1592, 1507, 1492 (benzene ring), 1271, 1239 (C-O-C), 1034 (C-O), 829 (*p*-substitution).

1,2-Bis{*N*-bis[4-(2-ethylhexyloxy)phenyl]amino-4-phenyl}ethane-1,2-dione (9): Aromatic 1,2-diketone derived from triphenylamine, Compound 9, is synthesized according to the same procedure as Compounds 2 and 5. The product is separated by column chromatography and chloroform as eluent to obtain a yellow solid in the yield of 41.3%. ^{1}H-NMR (400MHz, $CDCl_3$, δ): 7.72 (d, *J*=7.48Hz, 4H), 7.08 (d, *J*=8.84Hz, 8H), 6.88 (d, *J*=8.92Hz, 8H), 6.79 (d, *J*=9.0Hz, 4H), 3.83 (d, *J*=5.68Hz, 8H), 1.72 (m, 4H), 1.30-1.55 (m, 32), 0.93 (m, 24H). ^{13}C-NMR (101MHz, $CDCl_3$, δ): 193.51 (s) (carbonyl groups), 157.21 (s), 154.10 (s), 138.42 (s), 131.71 (s), 128.01 (s), 124.04 (s), 116.52 (s), 115.57 (s) (triphenylamine), 70.74 (s), 39.43 (s), 30.54 (s), 29.11 (s), 23.88 (s), 23.06 (s), 14.10 (s), 11.15(s) (2-ethylhexanyl groups). IR, υ_{max} (KBr, cm^{-1}): 3043 (ArH), 2966 (CH_3, υ_{as}), 2931 (CH_2, υ_{as}), 2864 (CH_2, υ_s), 1661 (C=O), 1592, 1499, 1464 (benzene ring), 1329 (CH_2, υ_s), 1285, 1234 (C-O-C), 1029 (C-O), 825 (*p*-substitution). ESI-MS (m/z): [M+1]=1057.7.

Bis{1,2-bis{*N*-bis[4-(2-ethylhexyloxy)phenyl]amino-4-phenyl}ethylene-1,2-dithiolate} nickel complex (10): Dithiolene nickel complex derived from triphenylamine, Compound 10, is synthesized according to the same procedure as Compounds 3 and 6. The product is separated by column chromatography and dichloromethane as eluent to obtain a blackish green solid in the yield of 21.3%. ^{1}H-NMR (400MHz, $CDCl_3$, δ): 7.23 (d, *J*=8.76Hz, 4H), 7.10 (d, *J*=8.84Hz, 8H), 6.88 (d, *J*=8.88Hz, 8H), 6.78 (d, *J*=8.76Hz, 4H), 3.84 (d, *J*=5.68Hz, 8H), 1.74 (m, 4H), 1.34-1.57 (m, 32H), 0.94 (m, 24H). ^{13}C-NMR (101MHz, $CDCl_3$, δ): 180.14 (s) (C=C), 156.72 (s), 149.83 (s), 140.17 (s), 133.96 (s), 130.21 (s), 127.75 (s), 118.48 (s), 115.73 (s) (triphenylamine), 71.10 (s), 39.87 (s), 30.95 (s), 29.52 (s), 24.28 (s), 23.46 (s), 14.50 (s), 11.55 (s) (2-ethylhexanyl groups). IR, υ_{max} (KBr, cm^{-1}): 3043 (ArH), 2957 (CH_3, υ_{as}), 2922 (CH_2, υ_{as}), 2854 (CH_2, υ_s), 1584, 1498, 1456 (benzene ring), 1345 (CH_2, υ_s), 1293, 1233 (C-O-C), 1293, 1233 (C=C), 1038 (C-O), 816 (*p*-substitution). ESI-MS (m/3z): [M/3]=745.4. Element. Anal. Calcd for $C_{140}N_4S_4H_{184}O_8Ni$: C, 75.17; N, 2.51; H, 8.23. Found: C, 74.75; N, 2.35; H, 8.21.

Filter fabrication: The NIR optical filters are fabricated by static solution-casting approach with polystyrene as transparent polymeric matrix and with dithiolene nickel complexes as NIR absorbing dyes. The specific procedure is given below: Polystyrene (1.0g) is firstly dissolved in chloroform and then dithiolene nickel complex (Compounds 3, 6 and 10, 1.0mg) synthesized by us is added into the chloroform solution of polystyrene. After stirring for 10 minutes, the composite solution is dropped on the glass substrate. With the solvent being dried spontaneously, a series of NIR optical filters are achieved respectively denoted as 3@PS for Compound 3, 6@PS for Compound 6 and 10@PS for Compound 10.

3. Results and Discussion

3.1. Synthesis

Dithiolene metal complexes generally conclude homoleptic complexes with a symmetrical molecular structure and heteroleptic complexes with an unsymmetrical molecular structure [28]. Heteroleptic dithiolene metal complexes are developed for nonlinear optical applications due to their noticeable first molecular hyperpolarizabilities[27], which are derived from the interligand charge transfer of HOMO-LUMO transition in unsymmetical molecules. As for absorbing dyes without any requirement of intramolecular hyperpolarization, homoleptic complexes are much more favored owing to their simple synthetic routes from symmetrical molecular structures. In view of DFT calculations on substituent effect for dithiolene metal complexes[18, 27-29], the electron-donating group increases the electron density of dithiolene moiety resulting in the higher energy levels of HOMO and LUMO. On account of much more improvement of HOMO, the band gap of dithiolene metal complexes will be decreased, i.e., the excitation energy of electrons from ligands to metal plane is reduced. In this case, the NIR absorption range of dithiolene metal complexes has a potential to be red-shifted through the introduction of electron-donating groups at the molecular periphery. Besides, the red-shift extent of NIR absorption range is decided by the electron-donating ability of substituents.

On the basis of molecular design strategy mentioned above, three

electron-donating groups, alkylcarbazole, alkylphenothiozine and dialkyltriphenylamide, are introduced into the molecular periphery of dithiolene nickel complexes as efficient electron-donating groups while the introduction of alkyl group is to increase the dye solubility. Carbazole, phenothiazine and triphenylamide, which are usually contained in organic compounds or conjugated polymers for organic photoelectronic semiconducting materials to improve the hole-transporting ability in organic light-emitting diodes, organic solar cells and organic field-effect transistors, are used to enhance the electron-donating ability of substituents at the molecular periphery affording the potential red-shift of NIR absorption range to biological optical window. The specific synthetic route is shown in **Scheme 1**. First of all, carbazole, phenothiazine and triphylamide are alkylated by 2-ethylhexylbromide to increase the molecular solubility, affording Compounds 1, 4 and 8. Then, three aromatic 1,2-diketones, Compounds 2, 5 and 9, are presented by acylation reaction of Compounds 1, 4 and 8 with oxalyl chloride. Finally, dithiolene nickel complexes, Compounds 3, 6 and 10, are synthesized under the action of P_2S_5 and $NiCl_2 \cdot 6H_2O$. The alkyl group, 2-ethylhexanyl group, is applied to increase the solubility of dithiolene nickel complexes in common solvents, which is a necessary issue for solution-processible molding approaches. As we expected, the resulting dithiolene nickel complexes have an excellent solubility in common solvents such as toluene, tetrahydrofuran, dichloromethane, chloroform and dioxane, except for N,N-dimethylformamide.

All the intermediates and target compounds are identified by $^{1}H/^{13}C$-NMR, IR and ESI-MS spectra. All the $^{1}H/^{13}C$-NMR spectra is carefully assigned as shown in **Figures S1-S18** of electronic supporting information (SI). The proton signals of carbazole ring in ^{1}H-NMR spectra of Compounds 1-3 are illustrated **Figure 1a**. Evidently, the singlet proton signal at 8.80 ppm, which is assigned to the protons marked out by two astisks in the molecular skeleton of Compound 2 in **Scheme 1**, appears in ^{1}H-NMR spectrum of Compound 2 compared with Compound 1. It is shifted again to the singlet proton signal at the high field of 8.48 ppm in ^{1}H-NMR spectrum of Compound 3. These results indicated the successful introduction of

carbonyl group into Compound 2 and its transformation in dithiolene nickel molecular core in Compound 3. The transformation of carbonyl group is further confirmed by the shift of carbon signal of carbonyl group from 195.08 ppm of Compound 2 to 181.80 ppm of Compound 3 in the ^{13}C-NMR sepctra of **Figure 1b**. In the process of ESI-MS measurement of Compound 2, the appearance of [M+1]=613.4 in **Figure S19** identifies the chemical structure of 1,2-diketone (M=612.4) instead of single ketone (M=584.4). The introduction and transformation of carbonyl group is also proved by the appearance of absorption peak at 1669 cm^{-1} in the IR spectrum of Compound 2 and by its disappearance in the IR spectrum of Compound 3 in **Figure 1c**. Finally, the appearance of [M+1]=1347.6 in the ESI-MS spectrum of **Figure S20** definitely proved the successful preparation of Compound 3, bis{1,2-bis[*N*-(2-ethylhexyl)-carbazol-3-yl]ethylene-1,2-ditholate} nickel complex. The measurement results of Compounds 3, 6 and 10 is in accord with their calculation values of C, N and H.

The changes of chemical shift of proton and carbon adjacent to carbonyl group in aromatic 1,2-diketones are also similarly found in ^{1}H/^{13}C-NMR spectra of Compounds 4-6 (^{1}H-NMR: 7.71ppm/singlet in Compound 5 to 7.40ppm/singlet in Compound 6; ^{13}C-NMR: 192.50ppm in Compound 5 to 179.32ppm in Compound 6; See. **Figures S6-S10**) and Compounds 8-10 (^{1}H-NMR: 7.72ppm/doublet in Compound 9 to 7.23ppm/doublet in Compound 10; ^{13}C-NMR: 193.51ppm in Compound 9 to 180.14ppm in Compound 10; See. **Figures S13-S18**). The appearance and disappearance derived from the introduction and transformation of carbonyl group are also revealed in the IR spectrum of Compounds 4-6 (1659 cm^{-1} in Compound 5, See. **Figure S21**) and Compounds 8-10 (1661 cm^{-1} in Compound 9, See. **Figure S22**). In addition, the introduction of 1,2-diketone into Compounds 5 and 9 is respectively verified by the signal of [M+1]=677.3 and [M+1]=1057.7 in the ESI-MS spectra of **Figures S23** and **S24**. The successful preparation of Compound 6, bis{1,2-bis[*N*-(2-ethylhexyl)-phenothiazin-3-yl]ethylene-1,2-ditholate} nickel complex, is further proven by the signal of [M+2]=1476.5 in the ESI-MS spectrum of **Figure S25**. Due to the large molecular weight of Compound 10, it is very difficult to

detect the signal of monocharged molecular ion (m/z) as above. Fortunately, its signal of triple charged molecular ion (m/3z=745.4), whose interval of isotopic ion peaks is approximately equal to 0.333, is found in its ESI-MS spectrum in **Figure 1d**. This result indicated the successful preparation of Compound 10, bis{1,2-bis{*N*-bis[4-(2-ethylhexyloxy)phenyl]amino-4-phenyl}ethylene-1,2-ditholate} nickel complex. The identification results of all the intermediates and target complexes are entirely in accord with the chemical structures in **Scheme 1**.

3.2. Thermal property

The thermal property of dithiolene nickel complexes is investigated by thermogravimetric analysis (TG) and differential scanning calorimetry (DSC). The TG curves in **Figure 2a** suggested that the onset degradation temperature of Compounds 3, 6 and 10 is respectively 413.1 ^{o}C, 339.7 ^{o}C and 391.3 ^{o}C, which is defined as the crosspoint temperature of two tangenthial lines at the onset degradation stage of TG curves as shown in **Figure 2a**. Evidently, dithiolene nickel complex derived from carbazole, Compound 3, bear the best thermal stability compared with Compounds 6 and 10. Except for that, TG curve of Compound 6 takes on an evident three-step degradation compared with Compounds 3 and 10. This point is derived from the introduction of phenothiazine ring, in which the sulphur atom is a main origination of thermal instability. The instable feature of sulphur atom in the phenothiazine ring is also shown in the lowest onset degradation temperature of Compound 6.

The DSC measurement in **Figure 2b** illustrated that the glass transition temperature of dithiolene nickel complexes is respectively 74.5 ^{o}C for Compound 3, 67.3 ^{o}C for Compound 6 and 93.8 ^{o}C for Compound 10. Except for the glass transition in the DSC curves of **Figure 2b**, Compound 3 has a recrystallization process at 148.3 ^{o}C with the enthalpy change of -26.45 J/g and a melting transition at 243.3 ^{o}C with the enthalpy change of 56.82 J/g and Compound 10 has two melting processes with the enthalpy changes of -4.315 J/g at 124.5 ^{o}C and -5.114 J/g at 142.7 ^{o}C. These results indicated that the resulting dithiolene nickel complexes bear a poor crystallinity, even

taking on a glassy state at low temperature due to the introduction of nonplane substituents such as phenothiazine, triphenylamide and 2-ethylhexanyl group.

XPS spectra

The chemical state of nickel, sulfur, nitrogen and carbon elements in dithiolene nickel complexes, Compounds 3, 6 and 10, is characterized in detail by X-ray photoelectron spectroscopy (XPS) with binding energies calibrated by that of C1*s*, which is an excellent tool to describe the chemical state of elements in organic or inorganic compounds and to provide the basic data about chemical bonds for theoretical calculation [30, 31]. The full-scale XPS spectrum of Compound 3 in **Figure 3a** obviously showed the signals of S2*p* (163 eV), N1*s* (400 eV), Ni2*p* (855 eV) and C1*s* (285 eV). These signals are also found in the full-scale XPS spectra of Compounds 6 and 10 (See. **Figures S26** and **S27**). The high-resolved XPS spectra of Ni2*p* in Compounds 3, 6 and 10 in **Figure 3b** showed that there is almost no change for chemical state of nickel in three dithiolene nickel complexes, suggesting that the stable binding energies of spin orbit splitting peaks (Ni2$p_{1/2}$ and Ni2$p_{3/2}$) with the approximate intensity ratio of $I_{p1/2}$:$I_{p3/2}$=1:2. It is speculated that the change of chemical states might happen in other elements of dithiolene nickel complexes. Therefore, the high-resolved XPS spectra of sulfur, nitrogen and carbon elements are also recorded to investigate their specific chemical states, which are involved in the change of electronic structure of dithiolene nickel complexes caused by the introduction of electron-donating groups at the molecular periphery.

The high-resolved XPS spectra of S2*p* in **Figure 3c** clearly indicated that the sulphur element in the molecular core of dithiolene nickel complexes takes on two chemical states at binding energies of 162.6 eV and 163.8 eV, without regard for the sulphur on phenothiazine ring at binding energy of 165.0 eV. By fitting their high-resolved XPS spectra (See. **Figures S28-S30**), the peak of S2*p* belonging to the molecular core is respectively divided into two evident individual peaks with different ratios (Compound 3: 50.7%@163.8eV, 49.3%@162.6eV; Compound 6: 86.7%@163.8eV, 13.3%@162.6eV; Compound 10: 65.0%@163.5eV;

35.0%@162.3eV. See. **Table S1**). This kind of dual-peak phenomenon was also discovered in other dithiolene nickel complexes approximately at 169 eV and 164 eV[32], even in Langmuir-Blodgett films of dithiolene nickel complex approximately at 168 eV and 163 eV[33]. The reference [33] thought the high binding energy at 168 eV is caused by the sulfur oxidation, i.e. S-O. Another explanation is that the existence of high binding energy at 169 eV is a kind of characteristic "satellite" feature of S2*p*[32], which is attributed to high oxidization degree and conjugation of anion moiety in the partially oxidized or charge transition species. The higher the degree of oxidation or conjugation, the higher is the degree of π-electron delocalization over the ligand through the π-d interaction, resulting in the more obvious "satellite" feature. Additionally, the sulphur in the molecular core of dithiolene nickel complex is proved to a mixture of 0 and -1 by different C-S stretching bands (1029 cm^{-1} and 1099 cm^{-1}) in IR spectra of original complex and by the deconvolution of high-resolved XPS spectrum of S2*s* in reduced complex at binding energy of 228 eV[34].

Our XPS result of high-resolved S2*p* is different from the outcoming in the references [32-34] although the coexistence of $[S]^0$ and $[S]^{-1}$ in dithiolene nickel complex is also confirmed. The dual-peak phenomenon appear approximately at low binding energies of 163.8 eV and 162.6 eV, which might be derived from the strong electron-donating ability of carbazole, phenothiozine and triphenylamide. Due to the stronger electron-donating ability of triphenylamide, the binding energies of $[S]^0$ and $[S]^{-1}$ are respectively decreased about 0.3 eV from Compounds 3 and 6 to Compound 10. In our case, the sulfur oxidation is definitely excluded due to the absence of O1*s* at binding energy of 531 eV in **Figure 3a**. Simultaneously, the binding energy of high-resolved N1*s* in **Figure 3d** has a minor shift on account of different electron-donating ability of carbazole, phenothiazine and triphenylamide in Compounds 3, 6 and 10. Besides, the binding energy of carbon element is unchangeable in the high-resolved C1*s* of **Figure 3f**, in which the shoulder appearance of C-O in Compound 10 with the content of 4.1% is also resolved out at binding energy of 286.5 eV by fitting its high-resolved C1s spectrum as shown **Figure**

S31. The data in **Table S1** showed a positive relationship between the content of $[S]^{-1}$ and the binding energy of N1*s*, indicating that the charge on $[S]^{-1}$ should come from nitrogen element on carbazole, phenothiazine and triphenylamide through electron π-delocalization. This point told us that the introduction of electron-donating groups has an extraordinary potential to modulate the electronic structure of dithiolene nickel complexes.

To the best of our knowledge, the chemical state of dithiolene ligand in metal complexes is still under debate to date[27, 28, 35], such as neutral dithioketone (L), radical monoanion ($L^{\bullet-}$) or dianionic dithiolate (L^{2-}) as shown in **Scheme 2**. Our XPS results related with the chemical state of S2*p* in the molecular core support the existence of radical monoanion [form d] in single dithiolene ligand. In consideration of unchangeable binding energy at 855.0 eV of high-resolved Ni2*p* in **Figure 3b**, the potential existence of neutral dithioketone (form a) and dianionic dithiolate (form b) is excluded since the single chemical state of Ni2*p* and the dual-peak phenomenon of S2*p* show the existence of the Ni^{2+} instead of the coexistence of Ni^{2+} and Ni^{0}/Ni^{4+}. According to the ratio of $[S]^{0}$:$[S]^{-1}$=1.03 in Compound 3, we know that the molecular core of dithiolene nickel complex derived from alkylcarbazole only take a radical monoanion (form d). Compound 6 takes a majority of overall π-electron delocalization (form c) owing to its ratio of $[S]^{0}$:$[S]^{-1}$=6.52. The molecular core of Compound 10 takes a part of radical monoanion due to its ratio of $[S]^{0}$:$[S]^{-1}$=1.86. These results told us that the chemical state of S2*p* in dithiolene ligand depends to a large extent on the electron-donating ability of substituents at the molecular periphery.

3.4. Electrochemical and optical properties

Cyclic voltammetry (CV) is carried out at a scanning rate of 100mv/s to investigate the electronic structure of dithiolene nickel complexes, especially the energy level of HOMO and LUMO, with the *n*-$BuNPF_6$ acetonitrile solution (0.1mol) as an electrolyte, with platinum carbon electrodes as working electrodes and with Ag/AgCl as reference electrode. The results indicated that Compounds 3, 6 and 10 exhibit an evident reversible reduction peak and a weak irreversible oxidation peak as

shown in the CV curve of Compound 10 of **Figure 4** (Compound 3: **Figure S32**; Compound 6: **Figure S33**). Based on the fact of reproduced CV curve in different loops, we deemed that the CV behavior of Compounds 3, 6 and 10 is reversible as a whole, i.e., the balance of gain and loss electron. Small irreversible oxidation wave is derived from the electron transportation through a conjugated bridge (-C=C-) from the donating-electron group at the molecular periphery to the molecular core. The ability of electron transportation results in the area of small oxidation wave, which is seemingly different for Compounds 3, 6 and 10 due to the different electron-donating ability of substituents at the molecular periphery, such as carbazole, phenothiazine and triphenylamine. The onset reduction potential (E_{red}^{onset}) of Compounds 3, 6 and 10 is respectively -0.73 V, -0.75 V and -0.79 V, whose energy level of LUMO is calculated with the formula E_{LUMO}=-(E_{red}^{onset}+4.44) eV to be -3.71 eV for Compound 3, -3.69 eV for Compound 6 and -3.65 eV for Compound 10. Similarly, the onset oxidation potential (E_{ox}^{onset}) of Compounds 3, 6 and 10 is respectively 0.55 V, 0.85 V and 0.60 V, whose energy level of HOMO is calculated with the formula E_{HOMO}=-(E_{ox}^{onset}+4.44) eV to be -4.99 eV for Compound 3, -5.29 eV for Compound 6 and -5.04 eV for Compound 10. Therefore, their electrochemical band gap (E_g^{el}) is calculated with the formula $E_g^{el} = E_{LUMO} - E_{HOMO}$ to be 1.26 eV for Compound 3, 1.60 eV for Compound 6 and 1.39 eV for Compound 10. It is obviously that the as-prepared dithiolene nickel complexes bear the typical characteristics of low band gap, suggesting their potentially excellent NIR absorption performance. All the CV data are summarized in **Table 1**.

The optical absorption property of dithiolene nickel complexes is measured using the dichloromethane solution with a concentration of 0.02 mg/mL as shown in the UV-vis-NIR spectra of **Figure 5a**. The results suggested that the absorption maximum (λ_{max}) of Compounds 3, 6 and 10 is respectively 1021 nm, 1088 nm and 1168 nm, where the molar extinction coefficient is calculated with the formula ε=A/bc to be

5.23×10^4 $L\cdot mol^{-1}\cdot cm^{-1}$ for Compound 3, 3.86×10^4 $L\cdot mol^{-1}\cdot cm^{-1}$ for Compound 6 and 5.81×10^4 $L\cdot mol^{-1}\cdot cm^{-1}$ for Compound 10. Here, ε is denoted to be the molar extinction coefficient; A is the absorbance; b is the thickness of quartz cuvette; c is the molar concentration. The absorption onset (λ_{onset}) wavelength is 1167 nm for Compound 3, 1295 nm for Compound 6 and 1387 nm for Compound 10. As a result, the optical band gap ($E_g^{op.}$) is calculated with the formula $E_g^{op.}=1240/\lambda_{onset}$ eV to be 1.06 eV for Compound 3, 0.96 eV for Compound 6 and 0.89 eV for Compound 10. All these results showed that the resulting dithiolene nickel complexes have an excellent NIR absorption performance as menthioned above. All the UV-vis-NIR data are listed in **Table 1**.

Evidently, the optical band gap is different from the electrochemical band gap as shown in **Table 1**, which is caused by different measurement mechanisms. The electrochemical energy level is determined through the electron achievement at LUMO and the losing at HOMO while the optical energy level stems from the photon excitation/recombination between HOMO and LUMO. As for Compounds 3, 6 and 10, the photons are basically excited from aromatic rings, which is proved by the existence of C_{KLL} Auger electron peak at binding energy of 1225 eV as shown in the inset of **Figure 3a** because the Auger electron peak is usually caused by the relaxation of atoms in excited state with photogenerated holes in the atomic internal electron shell[31]. Additionally, the dithiolene nickel complex derived from phenothiazine has the lowest of molar extinction coefficient as shown in **Table 1**, similarly to the lowest content of $[s]^{-1}$, the lowest binding energy of N1*s* and the lowest HOMO level. The reason is that the electrons are excited from HOMO not only in electrochemical measurement but also in the XPS measurement, even in electron π-delocalization. Therefore, the content of $[S]^{-1}$ in the molecular core has a direct relationship with both the binding energy of N1*s* and the oxidation potential, even the molar extinction coefficient. In addition, Compounds 3, 6 and 10 have a strong absorption property in the near-infrared region between 900 nm and 1300 nm, which is basically in accord with biological optical window (800~1300nm). This feature can be well applied to the

NIR optical filtering in biological optical window, even the NIR laser protection at 1064nm.

3.5. Near-infrared optical filter

In light of high molar extinction coefficient in the near-infrared region of dithiolene nickel complexes, a series of optical filters are fabricated on the glass substrate by solution-casting the concentrated solutions of polystyrene (PS) and Compounds 3, 6 and 10 in chloroform. The optical filters are denoted as 3@PS for Compound 3, 6@PS for Compound 6 and 10@PS for Compound 10. Here, PS is applied as polymeric matrix with an excellent optical transparency, whose transmittance is more than 90% in the visible and near-infrared light region as shown in **Figure 5b**. Notably, the optical filters are impossibly achieved with polymethylmethacrylate (PMMA) as a matrix, which is another universal transparent polymeric matrix for a variety of optical devices, due to the serious fading of Compounds 3, 6 and 10 in the near-infrared region as shown in **Figure S34**. This might be resulted from the degradation action of carbonyl groups in PMMA on dithiolene nickel complexes, which is found through the poor solubility of Compounds 3, 6 and 10 in DMF and the considerable blue-shift of absorption maxima in the DMF solution, for example, the large blue-shift of absorption maximum of Compound 10 from 1168 nm in dichloromethane to 1025 nm in DMF in **Figure S35** while the molar extinction coefficient at the absorption maximum is decreased about one order of magnitude from 5.81×10^4 $L\cdot mol^{-1}\cdot cm^{-1}$ in dichloromethane to 4.53×10^3 $L\cdot mol^{-1}\cdot cm^{-1}$ in DMF. Simultaneously, we also make an attempt to fabricate the optical filters through *in-situ* bulk polymerization with styrene as a monomer and with azodiisobutyronitrile (AIBN) as an initiator. Unfortunately, this experiment is also ended in failure owing to the rapid fading of dithiolene nickel complexes, which might be derived from the polymerization inhibition of sulphur-containing compounds on free radicals or the coordination action of vinyl groups with dithiolene nickel complexes having been applied to the initiators of polymerization reaction of vinyl monomers[36, 37] and the purification of olelifins[38]. Fortunately, the static

solution-casting approach is successful applied to fabricate the NIR optical filters from Compounds 3, 6 and 10 with PS as polymeric matrix. The transmittance spectra of optical filters are investigated and illustrated in **Figure 5b**. The results indicated that all the optical filters have an extraordinary ultraviolet absorption property, together with an NIR filtering region (See. **Table S2**, 885-1135 nm for 3@PS, 947-1214 nm for 6@PS and 986-1305 nm for 10@PS) and an transparent region (See. **Table S2**, 472-848 nm for 3@PS, 522-896 nm for 6@PS and 497-925 nm for 10@PS). These results suggested that 3@PS, 6@PS and 10@PS have the potential application in the NIR optical filtering performance within biological optical window, especially the NIR laser protection at 1064 nm.

3.6. Near-infrared laser protection

The performance of NIR laser protection is detailedly investigated by the laser transmittance measurement of NIR optical filters fabricated from dithiolene nickel complexes at the wavelength of common NIR lasers, such as 780, 1064 and 1550 nm. Their curves of transmitted laser power *versus* incidence laser power are illustrated in **Figure 6** and the laser transmittances are summarized in **Table S3**. The results in **Figure 6a** showed that the transmitted laser powers at 780nm of 3@PS, 6@PS and 10@PS are respectively 67.5%, 25.8% and 46.0%, which are less than their transmittances of 78.5%, 71.8% and 62.2% in the UV-vis-NIR spectra of **Figure 5a**. The measurement of transmitted laser power at 1064 nm in **Figure 6b** indicated that all the NIR optical filters have a low optical laser transmittance, which is respectively 5.7% for 3@PS, 9.7% for 6@PS and 8.3% for 10@PS. Their optical densities (OD) are calculated with the formula $OD=\lg(1/T)$ to be 1.24 for 3@PS, 1.01 for 6@PS and 1.08 for 10@PS, here, T is the laser power transmittance. It is believed that their optical density at 1064nm has a large potential to be further improved with the increase of dye-doping concentration. In addition, their transmitted laser powers at 1550nm are more than 80% as shown in the inset of **Figure 6b**. Obviously, the resulting dithiolene nickel complexes possess an excellent NIR laser protection performance at 1064nm. Other applications of these NIR absorbing dyes are under

research in our laboratory.

4. Conclusion

Soluble dithiolene nickel complexes are designed and synthesized as NIR absorbing dyes through the introduction of strong electron-donating groups at the molecular periphery. The resulting complexes are characterized by $^{1}H/^{13}C$-NMR, IR, ESI-MS, UV-vis-NIR and XPS spectra, together with TG, DSC and CV. The identification results are in accord with their chemical structures. The TG and DSC measurement indicated that the dithiolene nickel complexes have an excellent thermal stability, even taking on a glassy state at low temperature. The XPS results suggested that the dithiolene ligands in carbazole-containing nickel complex take a radical monoanion, depending to a large extent on the electron-donating ability of substituents at the molecular periphery. The content of $[S]^{-1}$ in the molecular core has a direct relationship with both the binding energy of N1*s* and the oxidation potential, even the molar extinction coefficient because the electrons are excitated from HOMO not only in electrochemical measurement but also in the XPS measurement, even in electron π-delocalization. The NIR optical filters could be fabricated through static solution-casting approach with polystyrene as transparent polymeric matrix and with dithiolene nickel complexes as NIR absorbing dyes. The laser transmittance measurement suggested that the fabricated NIR absorbing filters bear a good NIR optical protection performance at 1064 nm.

Acknowledgements: This work is supported by the National Natural Science Foundation of China (NSFC, U1304212 and 21274133) and the Development Foundation for Distinguished Junior Researchers at Zhengzhou University (No. 1421320043).

Supporting Information: $^{1}H/^{13}C$-NMR spectra of Compounds 1-10 in **Figures S1-S18**; ESI-MS spectra of Compounds 2, 3, 5, 9 and 6 in **Figures S19**, **S20**, **S23**-**S25**; Full-scale XPS spectra of Compounds 6 and 10 in **Figure S26** and **S27**; Fitted XPS

spectra of high-resolved S2*p* of Compounds 3, 6 and 10 in **Figure S28-S30**; XPS data of fitted core-level S2*p*, N2*s* and C1*s* in **Table S1**; Fitted high resolution XPS spectra of C1*s* of Compound 10 in **Figure S31**; CV curves of Compounds 3 and 6 in Figure S32 and S33; Transmittance spectra of Compounds 3, 6 and 10 with PMMA as a matrix in **Figure S34**; UV-vis-NIR spectra of Compound 10 with a concentration of 0.02mg/mL in dichloromethane and DMF in **Figure S35**; Filtering and transparent regions of optical filters in **Table S2**; Laser transmittance of optical filters at 780nm, 1064nm and 1550nm in **Table S3**.

References:

[1] Hou CY, Duan YR, Zhang QH, Wang HZ, Li YG. Bio-applicable and electroactive near-infrared laser-triggered self-healing hydrogels based on graphene networks. J Mater Chem 2012; 22: 14991-6.

[2] Wu JL, Chen FC, Chuang MK, Tan KS. Near-infrared laser-driven polymer photovoltaic devices and their biomedical applications. Energ Environ Sci 2011; 4: 3374-8.

[3] Maggio S, Zhang QN, Zhao ZX. Free-space optical backplane prototype for telecommunication equipment in the petabit/s range. Bell Labs Tech J 2013; 18: 285-91.

[4] Bigo S. Multiterabit/s DWDM terrestrial transmission with bandwidth-limiting optical filtering. IEEE J Sel Top Quant 2004; 10: 329-40.

[5] Sargent RB, O'Brien NA. Dielectric materials for thin-film-based optical communications filters. MRS Bull 2003; 28: 372-6(+344).

[6] Simi C, Dixon R, Schlangen M, Winter E, Lasota C. Night Vision Imaging Spectrometer (NVIS) processing and viewing tools. Proc SPIE 2001; 4381: 118-28.

[7] Kobrinski H, Cheung KW. Wavelength-tunable optical filters: Applications and technologies. IEEE Commun Mag 1989; 27: 53-63.

[8] Valery VT. Handbook of Coherent-Domain Optical Methods (2nd ED)-Biomedical Diagnostics, Environmental Monitoring, and Materials Science:

Fourier Transform Light Scattering of Tissues, Springer Science+Business Media New York, 2013. ISBN: 978-1-4614-5175-4 (Print), 978-1-4614-5176-1 (Online).

[9] Huang ZL, Chen SH, Lv CH, Huang Y, Lai JJ. Infrared characteristics of VO_2 thin films for smart window and laser protection applications. Appl Phys Lett 2012; 101: 191505 (1-4).

[10] Pansare VJ, Hejazi S, Faenza WJ, Prud'Homme RK. Review of long-wavelength optical and NIR imaging materials: Contrast agents, fluorophores, and multifunctional nano carriers. Chem Mater 2012; 24: 812-27.

[11] Luo SL, Zhang EL, Su YP, Cheng TM, Shi CM. A review of NIR dyes in cancer targeting and imaging. Biomaterials 2011; 32: 7127-38.

[12] Zhao LZ, Peng JJ, Huang Q, Li CY, Chen M, Sun Y, Lin QN, Zhu LY, Li FY. Near-Infrared Photoregulated Drug Release in Living Tumor Tissue via Yolk-Shell Upconversion Nanocages. Adv Funct Mater 2014, 24, 363-71.

[13] Yang JP, Shen DK, Zhou L, Li W, Li XM, Yao C, Wang R, El-Toni AM, Zhang F, Zhao DY. Spatially confined fabrication of core-shell gold nanocages@Mesoporous silica for near-infrared controlled photothermal drug release. Chem Mater 2013; 25: 3030-7.

[14] Cao J, Huang SS, Chen YQ, Li SW, Li X, Deng DW, Qian ZY, Tang LP, Gu YQ. Near-infrared light-triggered micelles for fast controlled drug release in deep tissue. Biomaterials 2013; 34: 6272-83.

[15] Chang YT, Liao PY, Sheu HS, Tseng YJ, Cheng FY, Yeh CS. Near-Infrared light-responsive intracellular drug and sirna release using au nanoensembles with oligonucleotide-capped silica shell. Adv Mater 2012; 24: 3309-14.

[16] Kuo TR, Hovhannisyan VA, Chao YC, Chao SL, Chiang SJ, Lin SJ, Dong CY, Chen CC. Multiple release kinetics of targeted drug from gold nanorod embedded polyelectrolyte conjugates induced by near-infrared laser irradiation. J Am Chem Soc 2010; 132: 14163-71.

[17] Yang XB, Zhang SX, Yang B, Wang CY, Ding ST, Wang AB. Research progress on near-infrared absorbing croconaine dyes for 1064nm laser protection. J Funct Mater 2013; 44: 3235-8.

[18] Miao QQ, Gao JX, Wang ZQ, Yu H, Luo Y, Ma TL. Synthesis and characterization of several nickel bis(dithiolene) complexes with strong and broa near-IR absorption. Inorg Chim Acta 2011, 376, 619-627.

[19] Men JF, Chen ZH, Cheng HF, Chu ZY. Night vision imaging system (NVIS) compatibility of cyanine dye-based NIR absorbing filter. Acta Optica Sinica 2008; 28: 1783-7.

[20] Wakita J, Kawamata S, Murano T, Fukamachi H, Hayasaka S. "Night view system" with pedestrian detection using near-infrared light. 15th World Congress on Intelligent Transport Systems and ITS America Annual Meeting 2008; 7: 4459-68.

[21] Morris JB, Fiddy MA, Pommet DA. Nonlinear filtering applied to single-view backpropagated images of strong scatterers. J Opt Soc Am A 1996; 13: 1506.

[22] Hamed AB, Mahdi HK, Farhad M. WDM and DWDM optical filter based on 2D photonic crystal Thue-Morse structure. Optik 2013; 124: 4416-20.

[23] Debnath K, Welna K, Ferrera M, Deasy K, Lidzey DG, O'Faolain L. Highly efficient optical filter based on vertically coupled photonic crystal cavity and bus waveguide. Opt Lett 2013; 38: 154-6.

[24] Yu JH, Han YQ, Huang HK, Li HZ, Hsiao VKS, Liu WP, Tang JY, Lu HH, Zhang J, Luo YH, Zhong YC, Zang ZG, Chen Z. All-optically reconfigurable and tunable fiber surface grating for in-fiber devices: A wideband tunable filter. Opt Express 2014; 22: 5950-61.

[25] Bruno B, Fabien L, Michel C, Michel L. Manufacturing of an absorbing filter controlled by a broadband optical monitoring. Opt Express 2008; 16: 12008-17.

[26] Shou CH, Luo ZY, Wang T, Shen WD, Rsengarten G, Wei W, Wang C, Ni MJ, Cen KF. Investigation of a broadband TiO_2/SiO_2 optical thin-film filter for hybrid solar power systems. Appl Energ 2012; 92: 298-306.

[27] Paola D, Luca P, Davide E, Mercuri ML, Angela S. Square-planar d^8 metal mixed-ligand dithiolene complexes as second order nonlinear optical chromophores: structure/property relationship. Coordin Chem Rev 2010; 254: 1434-47.

[28] Benedicte GDB, Kathleen IMCC, Fabienne A, Bui TT, Lydie V. Neutral d^8 metal bis-dithiolene complexes: synthesis, electronic properties and applications. Coordin Chem Rev 2010; 254: 1457-67.

[29] Soras G, Psaroudakis N, Manos MJ, Tasiopoulos AJ, Liakos DG, Mousdis GA. Synthesis, experimental and theoretical investigation of a new type nickel dithiolene comoplex. Polyhedron 2013; 62: 208-17.

[30] Sarma DD, Santra PK, Mukherjee S, Nag A. X-ray photoelectron spectroscopy: A unique tool to determine the internal heterostructure of nanoparticles. Chem Mater 2013; 25: 1222-32.

[31] Seah MP. Reference data for Auger electron spectroscopy and X-ray photoelectron spectroscopy combined. Appl Surf Sci 1999; 144: 161-7.

[32] Liu SG, Liu YQ, Zhu DB. Preparation and spectral properties of new molecular conductors based on anion salt. Synthetic Met 1997; 89: 187-91.

[33] Yang DD, Sun Y, Guo Y, Da DA. X-ray photoelectron spectroscopy of nickel dithiolene complex Langmuir-Blodgett films. Appl Surf Sci 1999; 148: 196-204.

[34] Kambe T, Sakamoto R, Hoshiko K, Takada K, Miyachi M, Ryu JH, Sasaki S, Kim J, Nakazato K, Takata M, Nishihara H. π-Conjugated nickel bis(dithiolene) complex nanosheet. J Am Chem Soc 2013; 135: 2462-5.

[35] Schrauzer GN, Mayweg VP. Coordination compounds with delocalized ground states. Bisdithioglyoxalnickel and related complexes. J Am Chem Soc 1965; 20: 3585-92.

[36] Li D, Mohamed FS, Yang XZ, Alak A, Harrison DJ, Fekl U, Brothers EN, Hall MB. The mechanism of alkene addition to a nickel bis(dithiolene) complex: The role of the reduced metal complex. J Am Chem Soc 2012; 134: 4481-4.

[37] Fan YB, Hall MB. How electron flow controls the thermochemistry of the addition of olefins to nickel dithiolenes: Predictions by density functional theory. J Am Chem Soc 2002; 124: 12076-7.

[38] Wang K, Stiefel EI. Toward separation and purification of olefins using dithiolene complexes: An electrochemical approach. Science 2001; 291: 106-9.

Figrues and Tables

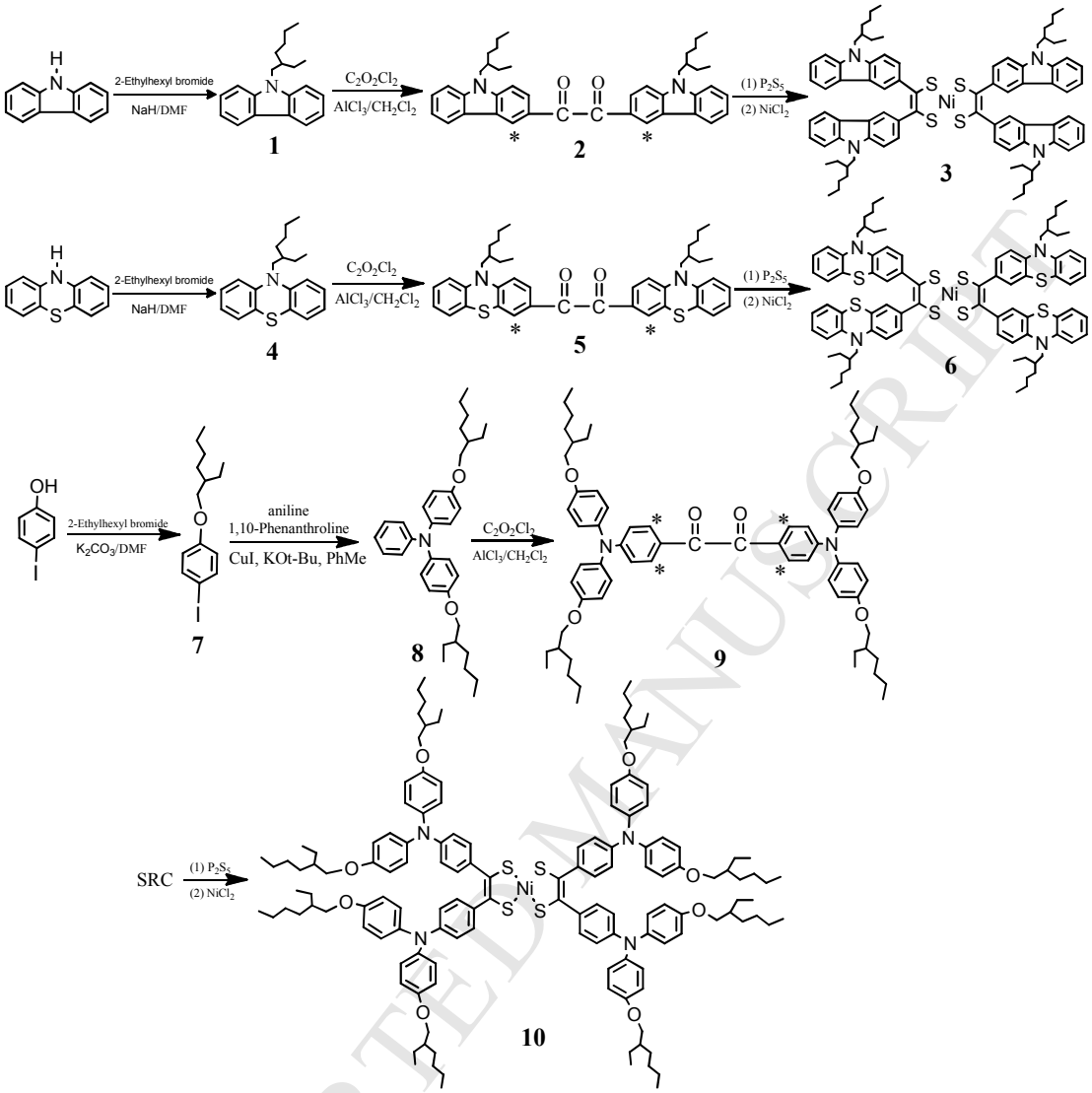

Scheme 1. Synthetic route of dithiolene nickel complexes.

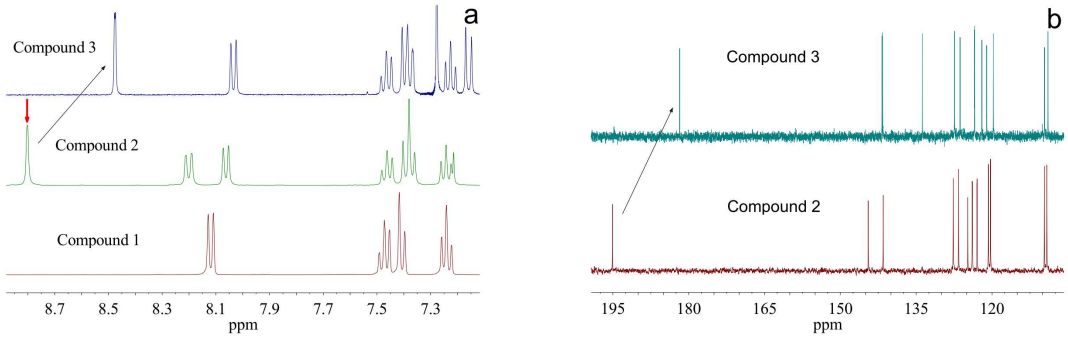

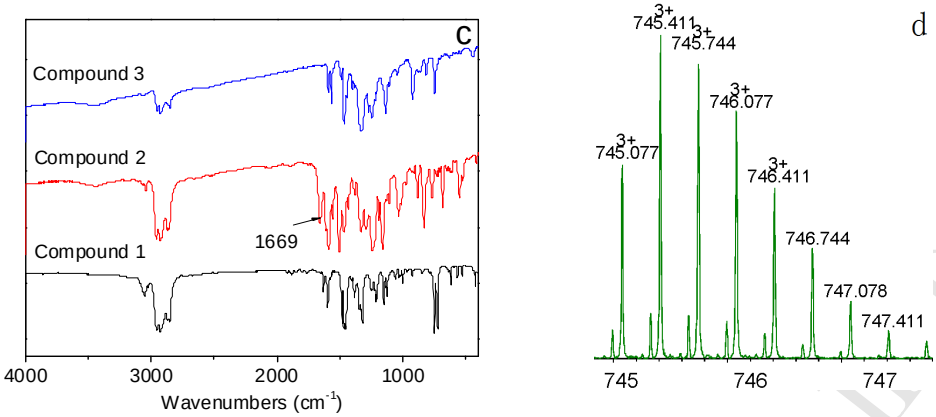

Figure 1. a) Proton signals of carbazole ring in ^{1}H-NMR spectra of Compounds 1-3; b) Carbon signals of carbazole and ethylene in ^{13}C-NMR spectra of Compounds 2 and 3; c) IR spectra of Compounds 1-3; d) Signals of triple charged molecular ion in the ESI-MS spectra of Compound 10.

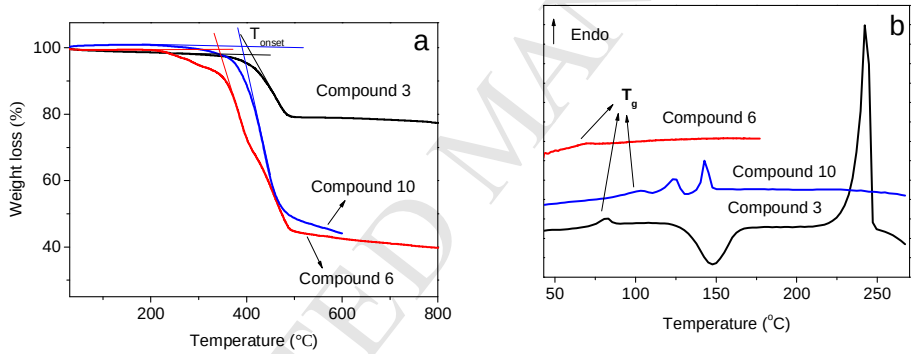

Figure 2. TG (a) and DSC (b) curves of Compounds 3, 6 and 10.

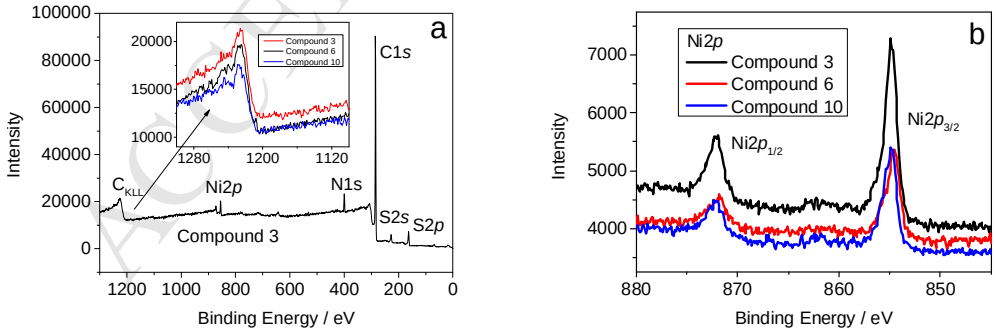

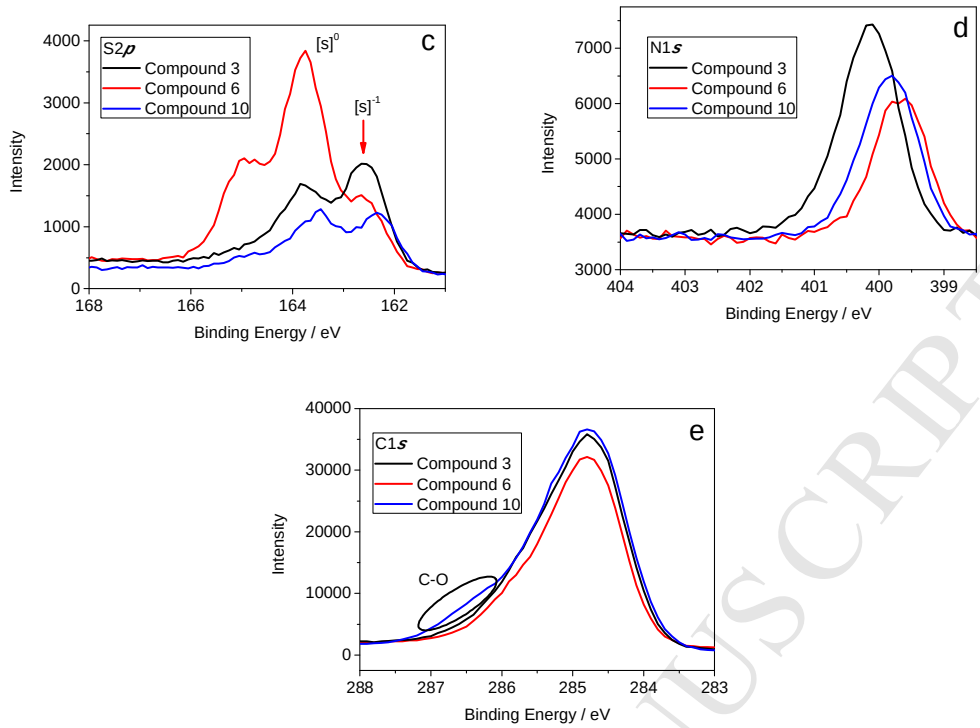

Figure 3. a) Full-scale XPS spectrum of Compound 3; b) High-resolved XPS spectra of Ni2*p* in Compounds 3, 6 and 10; c) High-resolved XPS spectra of S2*p* in Compounds 3, 6 and 10; d) High-resolved XPS spectra of N1*s* in Compounds 3, 6 and 10; e) High-resolved XPS spectra of C2*p* in Compounds 3, 6 and 10.

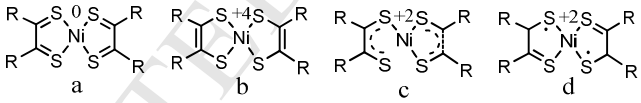

Scheme 2. Proposed chemical states of symmetrical dithiolene ligand (L, $L^{\bullet-}$, L^{2-}).

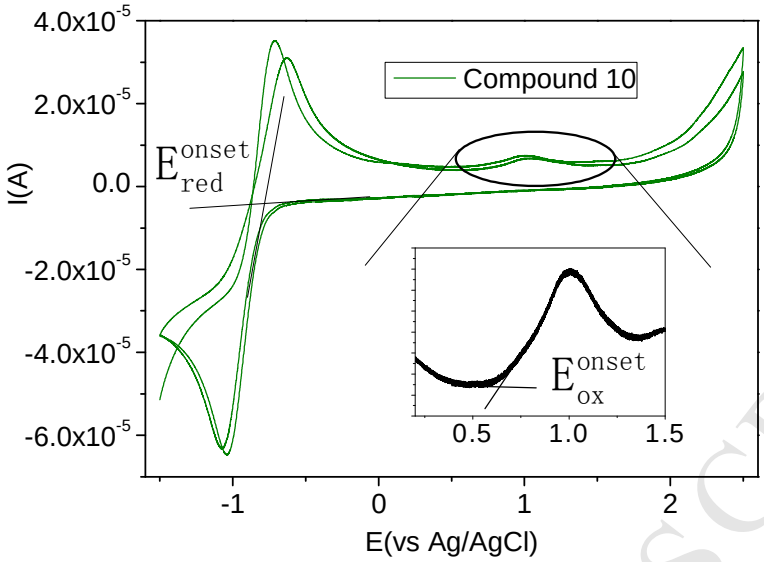

Figure 4. CV curve of Compound 10.

Table 1. CV and UV-vis-NIR data of dithiolene nickel complexes

Comp.s	E_{red}^{onset} /V	LUMO /eV	E_{ox}^{onset} /V	HOMO /eV	E_g^{el} / eV	λ_{max} / nm	ε/10^4L·mol^{-1}·cm^{-1}	λ_{onset} / nm	E_g^{op} / eV
3	-0.73	-3.71	0.55	-4.99	1.28	1021	5.23	1167	1.06
6	-0.75	-3.69	0.85	-5.29	1.60	1088	3.86	1295	0.96
10	-0.79	-3.65	0.60	-5.04	1.39	1168	5.81	1387	0.89

Note: E_{red}^{onset} is the onset reduction potential; E_{ox}^{onset} is the onset oxidation potential; E_g^{el} is the electrochemical band gap; ε is the molar extinction coefficient; λ_{onset} is the absorption onset wavelength; E_g^{op} is the optical band gap.

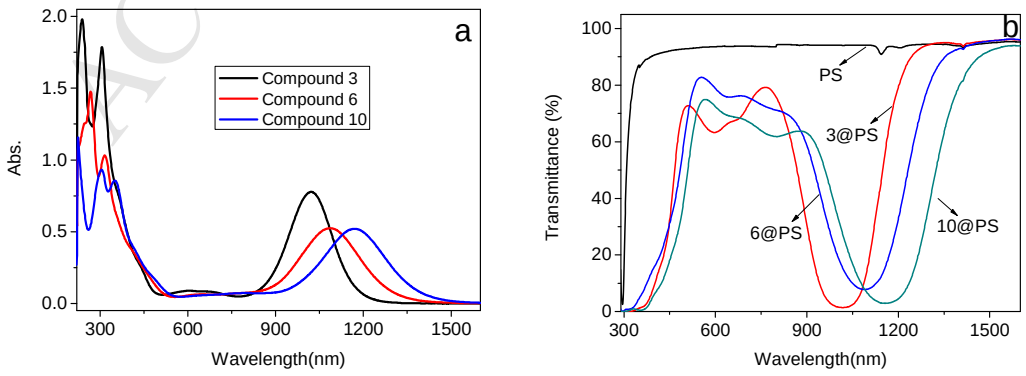

Figure 5. a) UV-vis-NIR spectra of Compounds 3, 6 and 10 in CH_2Cl_2; b) Transmittance spectra of Compounds 3, 6 and 10 with PS as matrix.

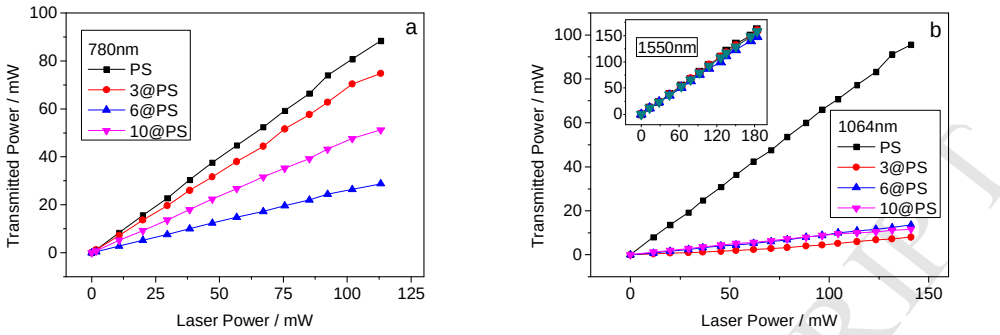

Figure 6. Transmitted power of optical filters at 780nm (a), 1064nm (b) and 1550nm (inset in b).

HIGHLIGHTS

1. Soluble dithiolene nickel complexes are synthesized as NIR absorbing dyes.
2. Dithiolene ligands in carbazole-containing nickel complex take radical monoanion.
3. Substituent electron-donating ability changes chemical state of molecular core.
4. The resulting complexes take on a glassy state at low temperature.
5. Dithiolene nickel complexes could be applied to NIR laser protection at 1064 nm.